

HELICOPTER CONTROL SYSTEM SYNTHESIS BY MULTIBODY MULTIDISCIPLINARY ANALYSIS

Pierangelo Masarati[†], Paolo Mantegazza
 Dipartimento di Ingegneria Aerospaziale, Politecnico di Milano,
 via La Masa 34, 20156 Milano, Italy

Pierre Abdel Nour, Claudio Monteggia
 AgustaWestland, Cascina Costa (VA), Italy

Reg Raval
 FHL A Claverham Division, Claverham, Bristol, England

Abstract

The paper presents a procedure for the synthesis of a rotorcraft aero-servo-elastic model, applied to the control system of a medium-weight helicopter tail rotor.

Symbols

A_p	actuator area
A_v	valve area
B_p	equivalent actuator damping
C_d	orifice flow coefficient
c_{ep}	external pressure loss coefficient
c_{ip}	internal pressure loss coefficient
D	actuator FRF denominator
F_l	external force applied to the piston
F_s	external force applied by the support
K	actuator support stiffness
k_c	valve flow-pressure coefficient
k_{ce}	valve overall pressure loss coefficient
k_i, k_f	valve input/output mechanical gains
k_q	valve flow gain
L	actuator length
M_p	piston mass
N_v, N_F	actuator FRF numerators
P	hydraulic fluid pressure
Q	hydraulic fluid volumetric flow
s	<i>Laplace's</i> variable
$V_{1,2}$	actuator chamber volumes
V_t	total actuator volume
x_i	valve input
x_p	piston (relative) displacement
x_s	actuator support displacement
x_v	valve opening
$Z(s)$	generic mechanical impedance
β_e	equivalent fluid bulk modulus
δ_{h_c}	hydraulic damping coefficient
ρ	hydraulic fluid density
$\omega_{h_{n,c}}$	(non-)centered hydraulic frequency

Introduction

The design of the hydraulic control system of a rotorcraft is traditionally accomplished by neglecting all interaction between the dynamics of the workload, in this case the rotor, and those of the hydraulic subsystem itself, relying on considerations related to the phase and gain margins of the isolated servo, under the assumption that the fundamental dynamics of the two subsystems are well separated. This may be true for conventional designs, where the cut frequency required by a normal control system is well below the lowest harmonics of the rotor and the hydraulic frequency of the actuator. However, Flight Control Systems (FCS) and Stability Augmentation Systems (SAS) require much higher cut frequencies that may well cause direct interaction of the control system with the lowest structural frequencies and with rotor harmonics; the interaction with the hydraulic frequency of the actuator should not be a concern except in very special cases; e.g. for large volume actuators or critical operating conditions, such as the partial failure of dual body actuators.

The dynamic system under analysis is made of two complementary parts, of equal importance: (a) a hydraulic actuator, and (b) an aeroelastic workload.

To this purpose, a conventional actuator model, as discussed in [1], is extended to consider arbitrary (i.e. non-centered) actuator positions, and selected non-linear contributions are added to account for effects such as friction and backlash.

[†]Corresponding author,

Tel.: +39 02 2399 8309

Fax: +39 02 2399 8334

E-mail: pierangelo.masarati@polimi.it

Presented at the European Rotorcraft Forum 2002
 Bristol (UK) 17–20 September 2002

On the side of the workload, while some important considerations can be drawn based on conventional Finite Element Analyses (FEA), e.g. the usual eigenanalyses of the mechanical system, the peculiar aeroelastic behavior of a helicopter rotor in different flight conditions requires more sophisticated analyses. The classical approach based on the use of comprehensive rotorcraft analysis codes may suffer from limitations when appropriate transfer functions of the aeroelastic rotorcraft system for the synthesis of the control system cannot be obtained; moreover, it is usually impossible to add the full nonlinear dynamics of the hydraulic control system to the rotorcraft model to verify the actual aeroservoelastic properties of the rotor.

A multibody multidisciplinary approach has been undertaken to exploit the capability of modern multibody formulations to account for exact kinematics description [2, 3], coupled to sophisticated structural flexibility models such as those commonly addressed, in the literature, as “exact” or “intrinsic” [4]. The multibody approach proved fundamental in analyzing sophisticated aeroelastic rotorcraft models in complex and unconventional operating conditions with no need to resort to undue simplifications [5, 6, 7, 8]. A multibody/multidisciplinary analysis code called MBDyn, based on an original formulation developed at the “Dipartimento di Ingegneria Aerospaziale” of the University “Politecnico di Milano”, has been used.

The multidisciplinary of the analysis tool is fundamental because while the synthesis and design phase are addressed by reducing the dynamics of the aeroelastic model to a state space model by system identification techniques, the assessment of the system is directly performed in the multibody framework by adding the hydraulic model, with full nonlinearities, to the aeroelastic system [9]. In both cases, the multibody approach naturally tends towards so-called virtual experimenting.

Description of the Problem

The proposed approach entails the two-way interaction between a detailed structural and aeroelastic model (which can be represented by any appropriate rotorcraft analysis tool, including conventional FEA for the structural part) with a detailed model of the hydraulic components, as summarized in Figure 1. Some linearized servoelastic analysis can be performed using conventional FEA tools; for instance, a linearized actuator has been added to the detailed FEM model (MSC/NASTRAN) by means of the general Transfer Function elements described in [10]. The linearization of both components of the aeroservoelastic system, either direct or by system identification,

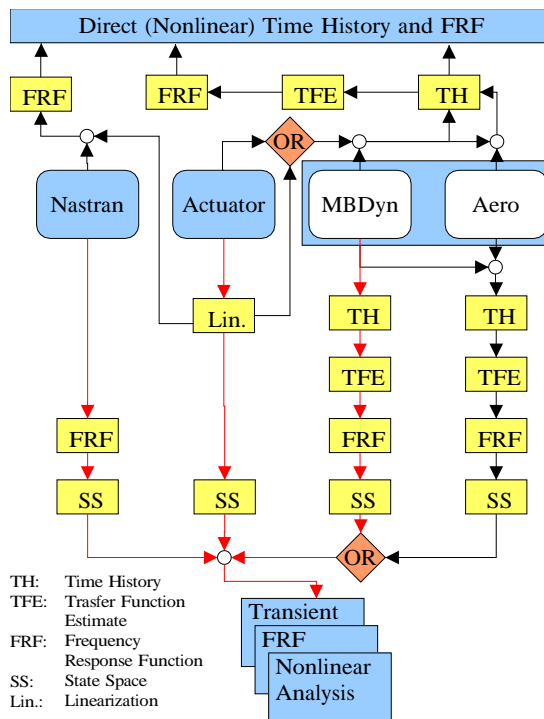


Figure 1: Modeling Approach

yields a reduced model that can be proficiently used in the design phase, while the integration of the hydraulic component into the aeroelastic analysis tool allows the direct simulation of the entire system.

Analysis Procedure

Referring to Figure 1, a model of the actuator (in the center) can be connected to a conventional FEM model (to the left) as well as to a multibody model (to the right) in different ways; the possible paths that can be followed are:

- downwards, to perform linear reduced model analyses in the frequency and in the time domain (possibly with selected nonlinearities in the latter case):
 - the linearized actuator model is augmented by a state-space model obtained by fitting the transfer function provided by the FE analysis of the system;
 - the linearized actuator model is augmented by a state-space model obtained by fitting an estimate of the transfer function obtained by analyzing the time histories provided by the multibody analysis;
- upwards, to perform direct analyses of the dy-

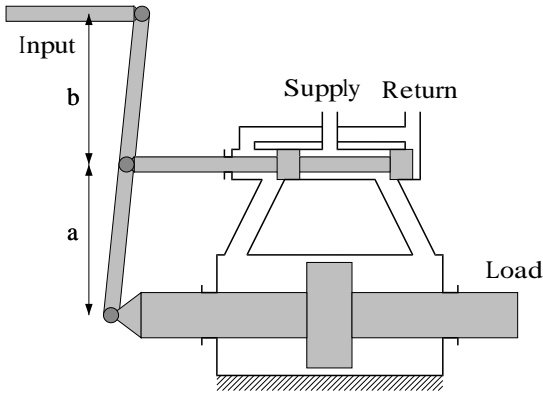


Figure 2: Actuator setup

dynamic system augmented by the actuator (both linearized or nonlinear):

- the linear FEM model is augmented by the linearized model of the actuator;
- the multibody model is augmented by the nonlinear actuator model to perform integrated time domain analyses.

In the present work the FEM paths were followed with structural models (usual FEM codes do not cope well with rotorcraft aeroelasticity) essentially to validate the structural multibody models and analyses were applicable. The work focuses on obtaining reliable reduced models from multibody analysis, while the integrated analysis of multibody models augmented by nonlinear hydraulic components is used to verify the reduced model analyses in off-design points.

Actuator Dynamics

The actuator and the spool valve that controls the flow in the chambers is usually described by means of a linearized model that captures its essential properties when it is subjected to displacements of limited amplitude about a reference position [1]. The actuator/valve setup is sketched in Figure 2. The flows through the valve are defined as:

$$Q_1 = k_q x_v - 2k_c P_1, \quad (1)$$

$$Q_2 = k_q x_v + 2k_c P_2. \quad (2)$$

The flow balance at the actuator chambers yields:

$$Q_1 - c_{ip}(P_1 - P_2) - c_{ep}P_1 = A_p \dot{x}_p + \frac{V_1}{\beta_e} \dot{P}_1 \quad (3)$$

$$-Q_2 + c_{ip}(P_1 - P_2) - c_{ep}P_2 = -A_p \dot{x}_p + \frac{V_2}{\beta_e} \dot{P}_2 \quad (4)$$

By defining the load flow, $Q_L = (Q_1 + Q_2)/2$, and the load pressure, $P_L = P_2 - P_1$, the piston force

balance equation,

$$M_p \ddot{x}_p = F_l - A_p P_L \quad (5)$$

after substituting the pressure and its time derivative from Equations (3, 4), and considering Equations (1, 2), results in an expression of the piston displacement, in the frequency domain, of the form:

$$x_p = \frac{N_v(s)}{D_p(s)} x_v + \frac{N_F(s)}{D_p(s)} F_l \quad (6)$$

The expressions of the numerators and of the common denominator are reported in Appendix A. By simple algebra manipulation, the fourth-order denominator can be cast in a form that shows a near-cancellation of the real pole with the zero of the valve numerator (which happens indeed in the centered case). The dominating second-order term of the denominator allows to infer an approximate form of the hydraulic frequency in the non-centered configuration:

$$\omega_{h_{nc}} \cong A_p \sqrt{\frac{\beta_e}{M_p} \left(\frac{1}{V_1} + \frac{1}{V_2} \right)}$$

which, in the centered case, becomes the usual

$$\omega_{h_c} = 2A_p \sqrt{\frac{\beta_e}{M_p V_t}}$$

The centered actuator condition is usually considered when designing a control system because it is expected to be the most critical; in fact, in this case both the hydraulic stiffness and damping show a minimum. When a mechanical feedback of the form $x_v = k_i x_i - k_f x_p$ is considered, Equation (6) becomes

$$x_p = \frac{k_i N_v(s)}{D_p(s) + k_f N_v(s)} x_i + \frac{N_F(s)}{D_p(s) + k_f N_v(s)} F_l \quad (7)$$

and the pole in zero disappears, so both the input-output and the dynamic compliance terms, respectively the first and the second right-hand members of Equation (7) admit a statical solution:

$$x_p(0) = \frac{k_i}{k_f} x_i(0) + \frac{k_{ce}/A_p^2}{k_v} F_l(0)$$

where the coefficients $k_v = (k_q/A_p)/k_f$ and $k_{ce} = (k_c + c_{ip} + c_{ep}/2)$ are related to essential dynamic properties of the actuator: k_v is the slope of the open-loop transfer function at low frequencies (a pure integrator), while k_{ce} is proportional to the damping of the hydraulic mode of the actuator:

$$\delta_{h_c} = \frac{k_{ce}}{A_p} \sqrt{\frac{\beta_e M_p}{V_t}}$$

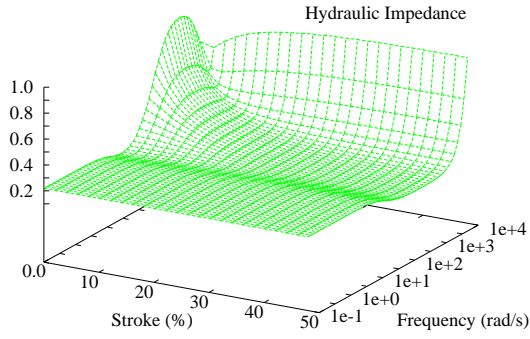


Figure 3: Hydraulic impedance with respect to frequency and stroke

Figure 3 shows the typical hydraulic impedance for a non-centered piston.

Practical Applications In practical applications, the piston equilibrium equation must be corrected by a dissipative effect, $-B_p \dot{x}_p$, related to the viscosity of the fluid leaking between piston and cylinder, and to generic dissipative effects; this contribution usually overruns the hydraulic damping. A significant effect may be introduced by the constraining of the actuator and of the control input; when a flexible support that allows a displacement x_s is considered, the piston equilibrium equation must be corrected by an inertial term of the form $-M_p \ddot{x}_s$, and the equilibrium equation of the actuator body must be added as well:

$$M_t \ddot{x}_s = F_s + F_l - M_p \ddot{x}_p$$

where M_t is the total mass of the actuator, since x_p is now the *relative* displacement of the actuator. The displacement of the support can be easily explicitated in the frequency domain:

$$x_s = \frac{F_s + F_l}{s^2 M_t} - \frac{M_p}{M_t} x_p$$

so the numerator of the compliance is fed-back and the total compliance is increased; the actuator and support are in series, so their compliances add.

Figures 4-5 show the input-output and the impedance of a linearized actuator both in open-loop and with a mechanical feedback; Figures 6-7 show the same plots in case a flexible support is considered as well.

Nonlinearities There are a few hidden nonlinearities even in this simplified scheme that are worth mentioning. First there is a dependency of the coefficients on the position of the piston that contributes to the vol-

ume of the actuator chambers, i.e.:

$$V_1 = V_{1_0} + A_p \left(\frac{L}{2} + x_p \right)$$

$$V_2 = V_{2_0} + A_p \left(\frac{L}{2} - x_p \right)$$

Moreover, the valve flow coefficient in a first approximation descends from a simplification of the generalization of *Bernoulli's* theorem applied to a turbulent incompressible fluid flowing from rest through an orifice (see [1]); assuming that the flow goes from a supply chamber at pressure P_0 to the actuator chamber at pressure p :

$$Q = C_d A_v \sqrt{\frac{2(P_0 - P)}{\rho}}$$

where C_d is a loss coefficient. The same applies to the other chamber, where the flow goes to the reservoir. The derivative of the flow with respect to the valve opening, x_v , yields the valve flow gain:

$$k_q = \frac{\partial Q}{\partial x_v} = C_d \frac{\partial A_v}{\partial x_v} \sqrt{\frac{2(P_0 - P)}{\rho}}$$

There is a dependency of the flow coefficient on the loading of the actuator: if the pressure in the actuator matches that of the supply, the system is in stall. If the valve opening is rectangular, the derivative of area with respect to the valve opening is the width of the valve orifice; otherwise a further nonlinear dependency on the valve opening results.

The derivative of the flow with respect to the pressure yields the flow-pressure coefficient:

$$k_c = \frac{\partial Q}{\partial P} = -\frac{C_d A_v}{\sqrt{2\rho(P_0 - P)}}$$

Again, there is a nonlinear dependency of the coefficient on the pressure and on the valve opening; in this case, the stall condition results in a singularity; in other words, this simplified model fails.

Multibody Multidisciplinary Model The above presented simplified models represent invaluable tools when designing hydraulic systems of practical use; however, when an integrated simulation of non-trivial transients of complex systems is addressed, more sophisticated and robust formulations must be used. Particular care must be taken to account for transition between different states (e.g., when transitioning from laminar to turbulent flow in pressure loss elements) or when reversing flows through valves, and so on. The multibody model includes pipelines with flow

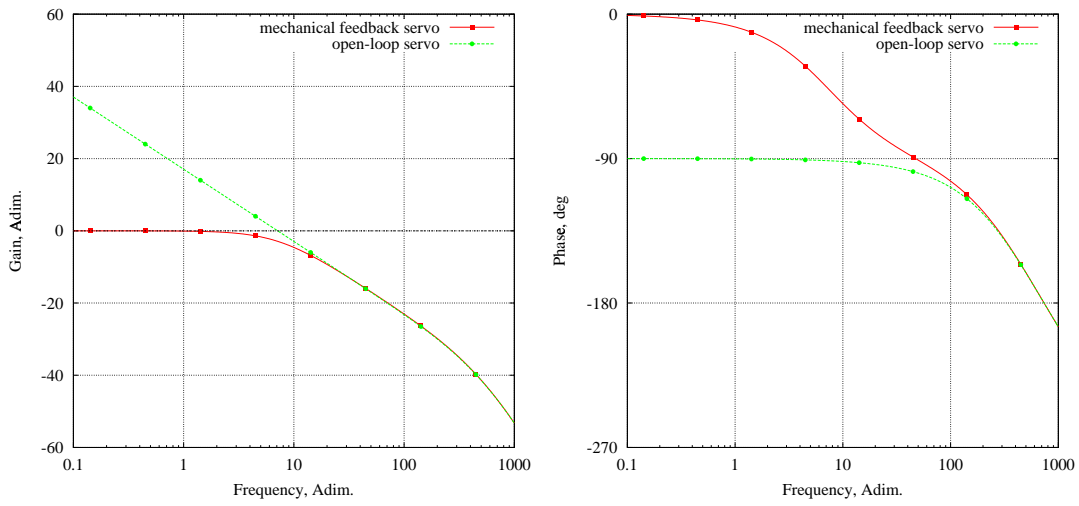


Figure 4: Amplitude/phase of control input/piston displacement

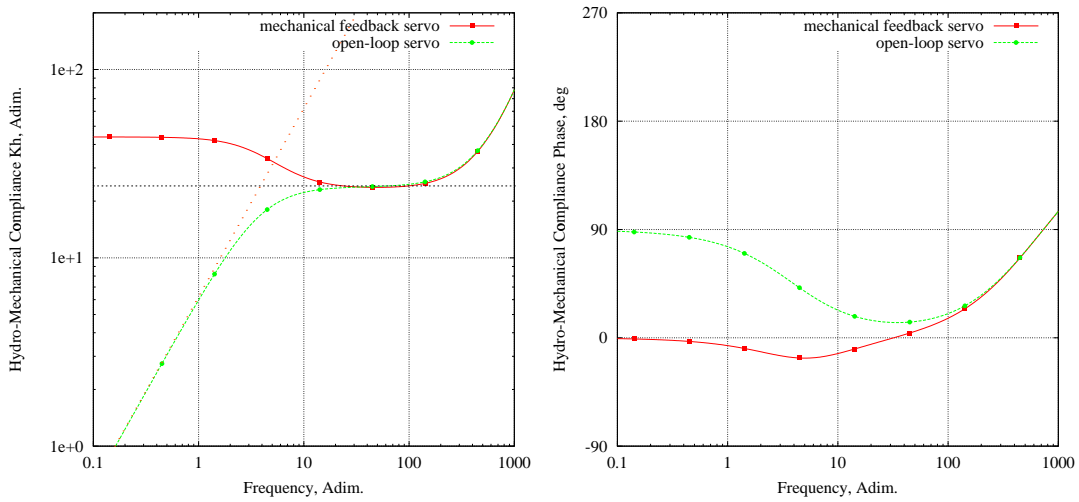


Figure 5: Amplitude/phase of the actuator impedance

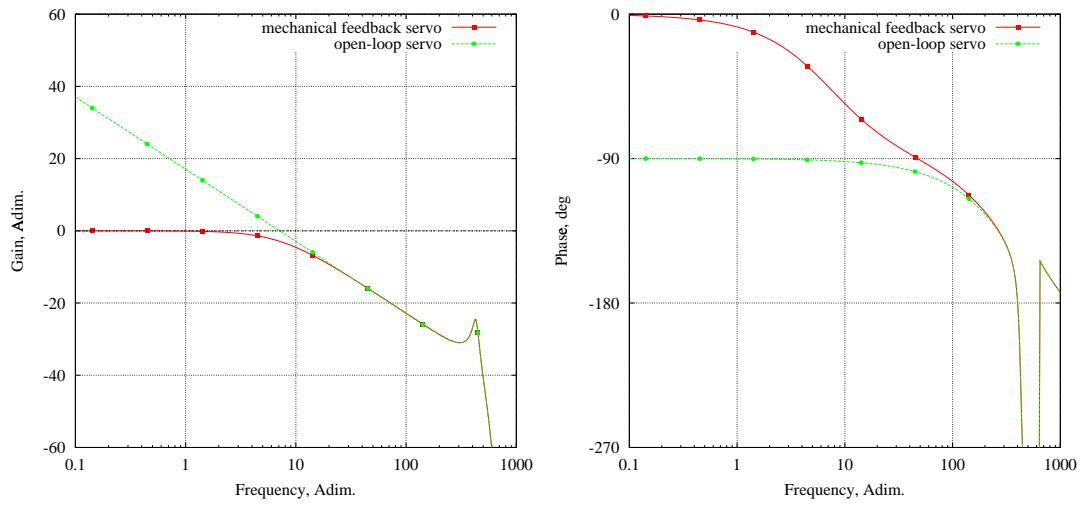


Figure 6: Amplitude/phase of control input/piston displacement; flexible support

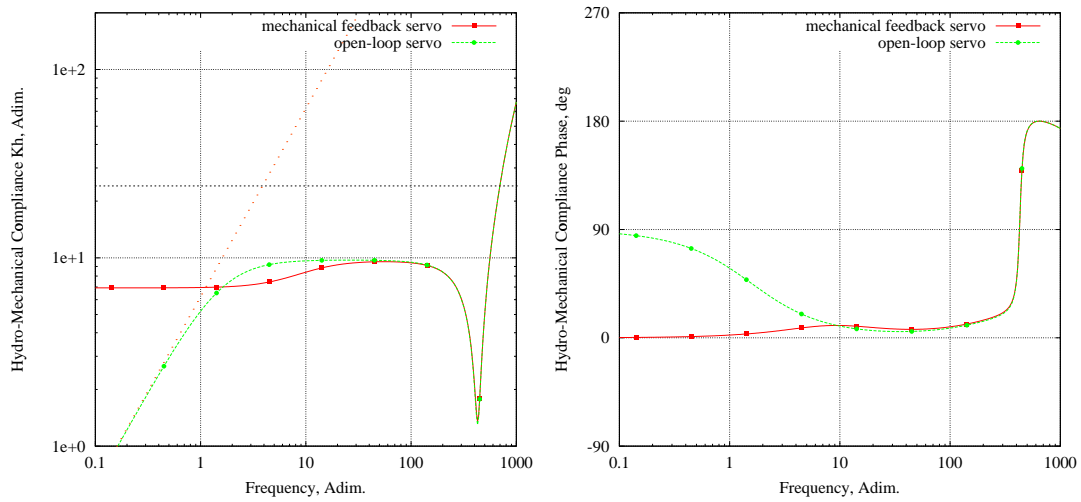


Figure 7: Amplitude/phase of the impedance of the system; flexible support

compressibility, lumped pressure losses, reservoirs, accumulators, ideal pressure and flow generators, ideal and dynamic control valves, pressure relief valves and actuators. By means of these basic building blocks and of special purpose elements, whenever appropriate, generic hydraulic circuits with arbitrary couplings to other physical environments (significantly mechanical systems and electric networks) can be modeled with the desired degree of refinement; see [9] for a more detailed description of the analysis capabilities. The nonlinear actuator can be attached to the structural and aeroelastic model of the rotor, or of the entire helicopter, to perform fully integrated transient analyses that go beyond usual frequency domain characterization and qualification of the hydraulic component.

State Space Realization The linearized actuator can be easily represented in the state space. Consider the states given by the pressures in the two chambers, P_1 and P_2 , the position and the velocity of the actuator, x_p and \dot{x}_p , and eventually those of the flexible support, x_s and \dot{x}_s ; the inputs to the system are the valve opening and the force acting on the piston:

$$\begin{aligned}\{x\} &= [P_1, P_2, x_p, \dot{x}_p, x_s, \dot{x}_s]^T \\ \{u\} &= [x_v, F_l]^T\end{aligned}$$

Without going into excessive detail about the contents of the matrices, a system of the form

$$\begin{aligned}\{\dot{x}\} &= [A]\{x\} + [B]\{u\} \\ \{y\} &= [C]\{x\} + [D]\{u\}\end{aligned}$$

results. This model is linear, with nonlinearities hidden in the system matrices; if reference values for the coefficients of the matrices are used, usual linear analyses in the time and in the frequency domain can be performed; in the time domain, nonlinear analyses can be performed as well. Other selected nonlinearities can be added, e.g. friction, backlash and freeplay in the valve and in the actuator, saturation, and more.

Workload Dynamics

The distinguishing aspect of the problem is the behavior of the workload. Its dynamics are added to the actuator model by applying the reaction force of the workload to the piston equation, i.e. by writing F_l in terms of the dynamics of the workload, which in turn may depend on the states of the actuator, significantly on the displacement of the piston, x_p . In the case under analysis, the procedure is applied to the control rod of the tail rotor of a medium-weight helicopter in two operating conditions: hover and forward flight at

cruise speed; a reference condition *in vacuo* is used to check whether the latter is overconservative with respect to the cases in air. The control rod of a tail rotor is attached to the piston, so the piston is loaded by the reaction of the aeroelastic system. Consider the transfer function of a mechanical system of the form

$$Z(s)x_p = F_l \quad (8)$$

which in principle may even comprise of a single mass, because the system is obtained by isolating everything that is upstream of the actuator:

$$s^2 M x_p = F_l$$

A state space realization of this system can be obtained by identifying a numerical or an experimental transfer function that describes the force generated by a prescribed displacement, velocity and acceleration time history of the piston. This can be directly obtained from many conventional finite element analysis codes (e.g. by means of MSC/NASTRAN) or by estimating the frequency response of the system when subjected to an appropriate excitation (e.g., white or colored noise, frequency sweep, impulsive load). The following solution was used in this work: a set of time responses of the multibody model of the tail rotor excited with colored noise (i.e. white noise with a low-pass filter with the cut frequency at $0.1\pi/\Delta t$) were used to estimate the transfer function of the system in Matlab by means of the `tfest` function. Then the `invfreqs` function was used to obtain a reduced order rational polynomial identification of the system, which was finally turned into a state space representation by means of the `tf2ss` function.

Multibody Aeroelastic Model A detailed multibody finite element model of the tail rotor under investigation was prepared, based on existing MSC/NASTRAN structural models (see Figure 8) and CAMRAD/JA aeroelastic models. The rotor is four bladed, soft-in-plane, with positive δ_3 ; the blades are straight, with constant chord; only a limited portion of the blade tip is swept backward. An elastomeric bearing is used to allow the pitch, flap and lag motions; there is an elastomeric lag damper. The pitch motion is controlled by means of a spider whose position is imposed by a non-rotating control rod inside the mast. The spider moves four pitch links that are attached behind the blade, at an inner radius with respect to the elastomeric hinges.

All of the above mentioned components were included in the multibody model, most of them as beam finite elements, with a high degree of refinement. Particular

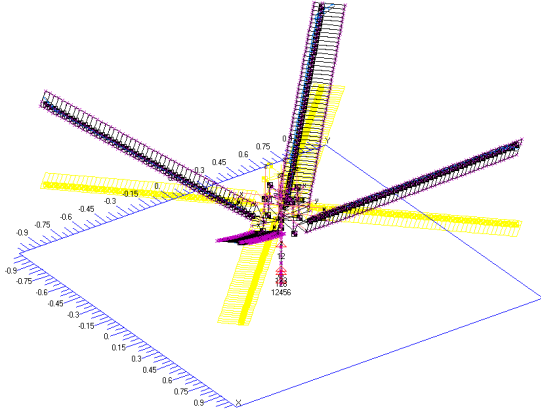


Figure 8: MSC/NASTRAN Model

care was dedicated to the modeling of the rotor blades and of the collective pitch control system, which significantly influences the impedance of the equivalent dynamic system that must be connected to the actuator.

A detailed description of the multibody model and of the validation procedure, mostly based on comparisons with the available MSC/NASTRAN and CAMRAD/JA analyses where applicable, is outside the scope of this paper.

Model Constraining As stated before, the analysis required a free model of the rotor; at least, the control rod had to be disconnected from the actuator. Since the transient analysis, for numerical reasons, must be performed by applying a force and measuring a displacement, this makes most of the analyses, especially those with aerodynamic loads, nearly unfeasible without an appropriate constraint. As a consequence, a modified procedure was required. Assuming that the dynamic system of Equation (8) is free, its transfer function can be written as $Z = s^2 \tilde{Z}$. The system must be loaded by an exciting force to determine its response in terms of displacement; however, while we need to measure the displacement, we do not want it to be too large, or to drift, because this would result in changing the reference conditions of the test. We can add a transfer function that statically constrains the system:

$$\left(W(s) + s^2 \tilde{Z}(s) \right) x_p = F_l$$

After the time response is obtained, the desired transfer function results from the identification of the force generated by the displacement x_p ; if the force F_l is used, the constrained system is identified; however, a force term $\tilde{F}_l = F_l - W(s)x_p$ can be used, assuming

the constraint transfer function $W(s)$ is known. This technique can also be used in the time domain; however, in this case a convolution is required: if $w(t)$ is the impulse response of the constraint, the corrected force in the time domain is

$$\tilde{F}_l(t) = F_l(t) - \int_0^t w(t-\tau) x_p(\tau) d\tau$$

which becomes significantly simple when the constraint is a simple spring and its impulse response is a *Dirac's* delta function, $w(t) = K\delta(t)$, i.e. the constraint represents a direct transmission term:

$$\tilde{F}_l(t) = F_l(t) - Kx_p(t)$$

Integrated Model Performances There are basically two modes that gain significant importance in the case under analysis. Obviously they are collective, because the others, i.e. the cyclic and the reactionless modes, do not affect the displacement of the control rod. One is mainly a rigid flapping mode, which shows some participation of the control displacement due to the strong pitch-flap coupling; however this mode does not show a significant participation to the dynamics of the aeroservoelastic system, possibly because the flapping motion is strongly damped by the aerodynamics. The second mode, whose frequency is about 4.5/rev, is the first rotor torsion mode. This is only slightly damped by the aerodynamics and involves a significant control rod displacement; it shows a large interaction with the actuator dynamics, as can be appreciated in Figures 9-10. If a model reduction based on physical parameters were required, leading to conventional rotor/control integration procedures, the rotor could be reduced to a single degree of freedom model by considering this mode only. However this assumption may be violated if a different system is considered, e.g. a main rotor, with a different control system, lower overall frequencies, and a higher modal density due to the interaction of the actuators with both collective and cyclic modes.

Figure 11 shows a comparison of the input-output transfer function with and without aerodynamic forces. The damping introduced by the aerodynamics is evident: a gain margin higher than 30 is available, instead of less than 10 as shown *in vacuo* on a higher mode. In both cases the phase margin (which is 45°, about the same in both cases), is sufficient.

Design Considerations

The integration of an actuator into a generic mechanical system requires some knowledge of its interaction

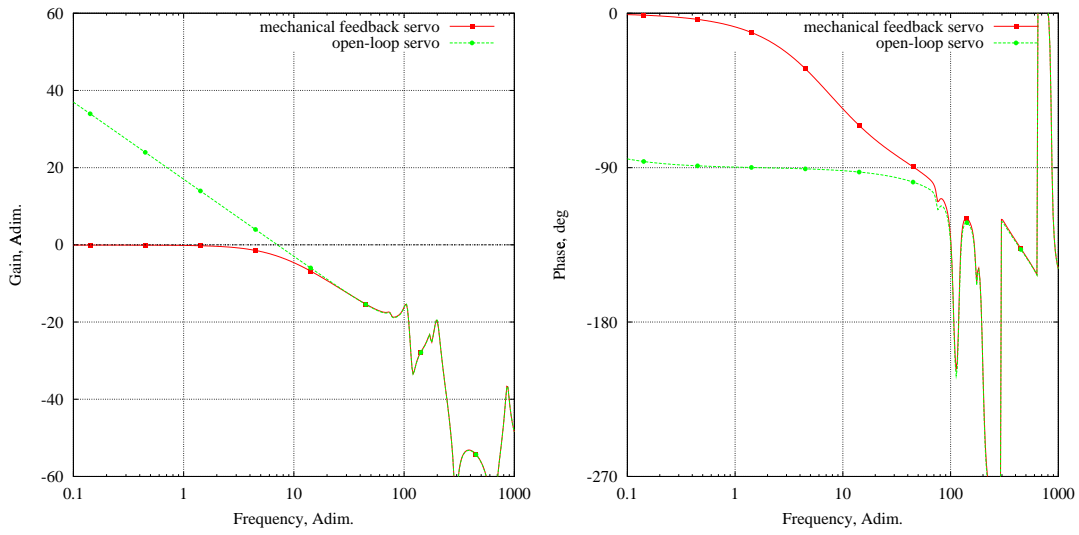


Figure 9: Amplitude/phase of control input/piston displacement; forward flight

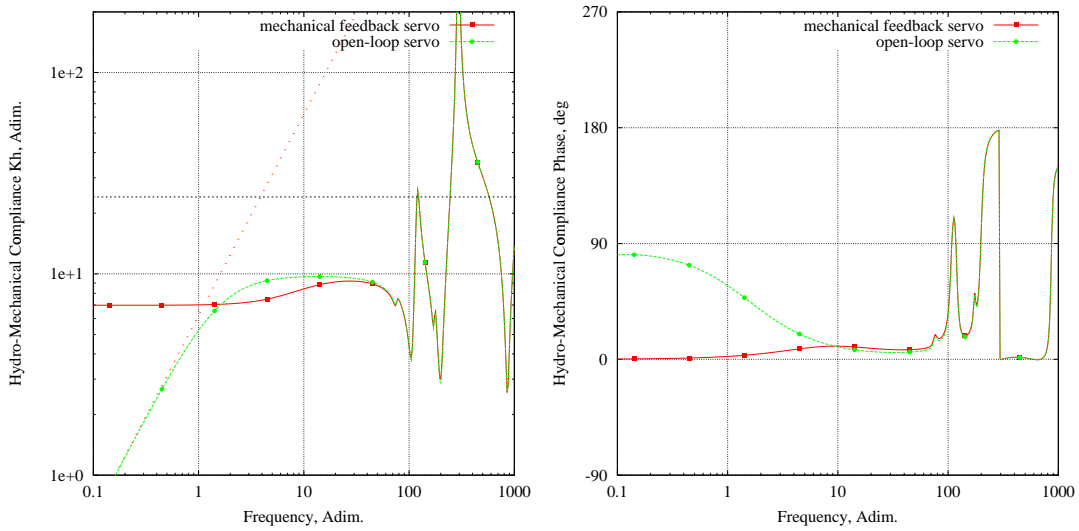


Figure 10: Amplitude/phase of the impedance of the system; forward flight

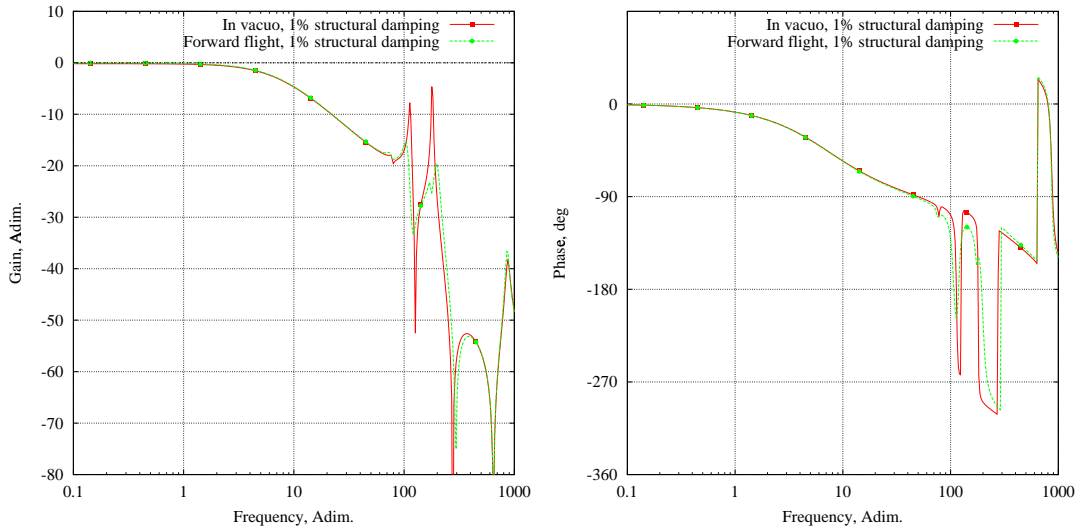


Figure 11: Amplitude/phase of control input/piston displacement; forward flight and in vacuo with 1% structural damping on control/blade collective twist mode

with the rest of the system. The design of such systems is usually performed as an iterative trial-and-error process. The main properties of an actuator for controlling the collective pitch of a tail rotor result from estimating a set of parameters; the same considerations apply to whatever system, including the control system of the main rotor, provided that appropriate generalizations are applied to the definitions of the properties. They can be grouped as:

- **geometry**: the geometry and the kinematic relationship between the parts of the system, e.g. the required stroke (or the collective pitch range) and the stroke/pitch ratio;
- **servo**: the properties of the servo-valve, i.e. the valve flow and pressure coefficients, mainly affecting the quasi-static response of the close-loop system;
- **environment**: fluid properties, e.g. the equivalent bulk modulus, the operating temperature which determines the viscosity;
- **loads**: the design and the dynamic loads the actuator must carry.

Most of these properties are closely related; some are usually given, e.g. the power supply pressure, unless special performance requirements determine the sizing of the hydraulic system. The latter points separates what are the design loads, namely the structural loads the actuator must carry, and the dynamic loads, i.e. the loads the actuator must carry while preserving the capability of accurately positioning the workload.

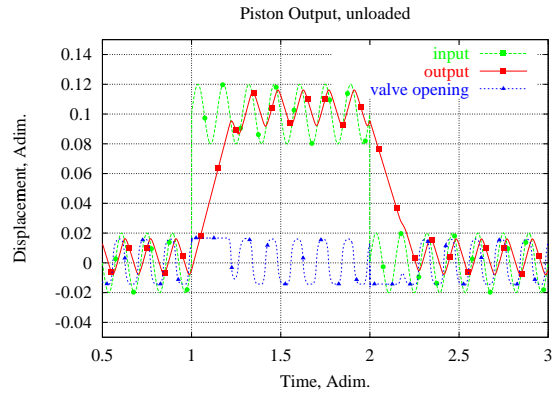


Figure 12: Input/output and valve opening time histories; unloaded system

In fact, it is reasonable to assume that the actuator, acting as a filter, can still provide some workload positioning even when subjected to high loads at frequencies far above the cut frequency. A usual actuator design requirement is to have a worst-case load pressure $P_L = P_1 - P_2$ that is about $2/3$ of the supply pressure $P_s \cong P_1 + P_2$. Actually, a dynamic load exceeding the supply pressure usually can be tolerated by an actuator, provided it acts at a frequency that is well above the cut frequency, as shown in Figures 12-13; they show the response of a fully nonlinear multibody model of the actuator subjected to a 2% amplitude harmonic desired input close to the cut frequency, plus a 10% amplitude step response, in case the system is unloaded or loaded by a harmonic force at 7 times the cut frequency, in case the average value is about 70%

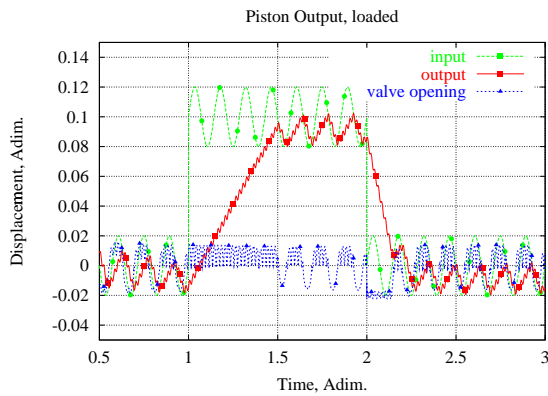


Figure 13: Input/output and valve opening time histories; loaded system

of the stall load and the dynamic amplitude is about 40% of the stall load, so that the peak amplitude exceeds 110% of the stall load. The valve opening is also shown. Note how the quality of the positioning is deteriorated by the loading; there is a significant saturation in the step response, which is emphasized in the loaded case. The harmonic response is highly deteriorated by the nonlinearities in the system, significantly by the quadratic pressure losses that are significant due to the amplitude of the displacements. The loaded case, however, still shows some residual positioning capability.

Concluding Remarks

A framework for the integrated analysis of multidisciplinary problems was presented; the framework was applied to the aeroservoelastic analysis of the interaction between rotor and control system dynamics of a conventional tail rotor. The rotor was modeled by means of a multibody multidisciplinary formulation that allows the integrated analysis of multiphysics problems in the same environment. The structural and aeroelastic models were validated by comparison with available results from conventional analysis tools, such as MSC/NASTRAN and CAMRAD/JA. The procedure entails the estimation and the identification of a set of transfer functions of the workload applied to the actuator, which were used in a state-space linearized model of the actuator for conventional frequency domain analysis and for time domain analysis, possibly considering selected nonlinearities. In a second phase, the nonlinear actuator was integrated into the multibody model to perform direct time domain analyses of the aeroservoelastic system. The multibody multidisciplinary approach yielded satisfactory results in comparison with more conventional analysis tools; its importance in evaluating off-design configurations proved invaluable.

Acknowledgements

This work has been supported by Agusta S.p.A. under Agusta Research Contract Order NN-000/1505; the Authors acknowledge the contributions of Prof. Ghiringhelli and Lanz and of Mr. Quaranta to the development of the multibody software.

References

- [1] H. E. Merritt, *Hydraulic Control Systems*. New York: John Wiley & Sons, 1967.
- [2] A. A. Shabana, *Dynamics of Multibody Systems*. Cambridge, MA: Cambridge University Press, 1998.
- [3] M. Geradin and A. Cardona, *Flexible Multibody Dynamics: a Finite Element Approach*. Chichester: John Wiley & Sons, 2001.
- [4] D. L. Kunz, "A survey and comparison of engineering beam theories for helicopter rotor blades," *Journal of Aircraft*, vol. 31, no. 3, pp. 473–479, 1994.
- [5] G. L. Ghiringhelli, P. Masarati, P. Mantegazza, and M. W. Nixon, "Multi-body analysis of a tiltrotor configuration," *Nonlinear Dynamics*, vol. 19, pp. 333–357, August 1999.
- [6] G. L. Ghiringhelli, P. Masarati, and P. Mantegazza, "A multi-body implementation of finite volume beams," *AIAA Journal*, vol. 38, pp. 131–138, January 2000.
- [7] G. Quaranta, P. Masarati, M. Lanz, G. L. Ghiringhelli, P. Mantegazza, and M. W. Nixon, "Dynamic stability of soft-in-plane tiltrotors by parallel multi-body analysis," in *26th European Rotorcraft Forum*, (The Hague, The Netherlands), pp. 60.1–9, 26–29 September 2000.
- [8] G. L. Ghiringhelli, P. Masarati, and P. Mantegazza, "Analysis of an actively twisted rotor by multibody global modelling," *Composite Structures*, vol. 52/1, pp. 113–122, April 2001.
- [9] P. Masarati, G. L. Ghiringhelli, M. Lanz, and P. Mantegazza, "Integration of hydraulic components in a multibody framework for rotorcraft analysis," in *26th European Rotorcraft Forum*, (The Hague, The Netherlands), pp. 57.1–10, 26–29 September 2000.
- [10] D. N. Hering, *MSC/NASTRAN Advanced Dynamics Analysis User's Guide*. U.S.A.: The MacNeal-Schwendler Corporation, 1997.

Appendix A

The numerators and the common denominator of Equation (6) are:

$$\begin{aligned}N_v(s) &= (V_t s + 4k_{cu}\beta_e) k_q \beta_e A_p \\N_F(s) &= V_1 V_2 s^2 + (k_{cu} + k_{ce}) \beta_e V_t s + 4k_{cu} k_{ce} \beta_e^2 \\D_p(s) &= s (M_p V_1 V_2 s^3 + (k_{cu} + k_{ce}) \beta_e M_p V_t s^2 + (4k_{cu} k_{ce} \beta_e^2 M_p + \beta_e A_p^2 V_t) s + 4k_{cu} \beta_e^2 A_p^2)\end{aligned}$$

where

$$\begin{aligned}k_{cu} &= k_c + \frac{c_{ep}}{2} \\k_{ce} &= \left(k_c + c_{ip} + \frac{c_{ep}}{2} \right)\end{aligned}$$